New Insight into Daptomycin Bioavailability and Localization in Staphylococcus aureus Biofilms by Dynamic Fluorescence Imaging

Rym Boudjemaa, Romain Briandet, Matthieu Revest, Cédric Jacqueline, Jocelyne Caillon, Marie-Pierre Fontaine-Aupart, Karine K. Steenkeste

New insight into daptomycin bioavailability and localization in *S. aureus* biofilms by dynamic fluorescence imaging.

Rym Boudjemaa,[a#] Romain Briandet,[b] Matthieu Revest,[c,d] Cédric Jacqueline,[d] Jocelyne Caillon,[d] Marie-Pierre Fontaine-Aupart,[a] and Karine Steenkeste[a]

Institut des Sciences Moléculaires d'Orsay (ISMO), CNRS, Univ. Paris-Sud, Université Paris-Saclay, F-91405 Orsay, France[a]; Micalis Institute, INRA, AgroParisTech, Université Paris-Saclay, 78350 Jouy-en-Josas, France[b]; CHU Rennes, Rennes, France[c]; Université de Nantes, Faculté de Médecine, UPRES EA 3826, Nantes, France[d]

Running head: daptomycin diffusion-reaction in *S. aureus* biofilms

#Address correspondence to Rym Boudjemaa, rym.boudjemaa@u-psud.fr

ABSTRACT

Staphylococcus aureus (S. aureus) is one of the most frequent pathogens responsible for biofilm-associated infections (BAI) and the choice of antibiotics to treat these infections remains a challenge for the medical community. In particular, daptomycin has been reported to fail against implant-associated *S. aureus* infections in clinical practice while its association with rifampicin remains a good candidate for BAI treatment. To improve our understanding of such resistance/tolerance toward daptomycin, we took advantage of the dynamic fluorescence imaging tools (time-lapse imaging and FRAP) to locally and accurately assess the antibiotic diffusion-reaction in methicillin-susceptible and methicillin-resistant *S. aureus* biofilms. To provide a realistic representation of daptomycin action, we optimized an *in vitro* model built on the basis of our recently published *in vivo* mouse model of prosthetic vascular graft infections. We demonstrated that at therapeutic concentrations, daptomycin was inefficient to eradicate biofilms while the matrix was not a shield to the antibiotic diffusion and to its interaction with its bacterial target. In the presence of rifampicin, daptomycin was still present in the vicinity of the bacterial cells allowing the prevention of the emergence of rifampicin-resistant mutants. Conclusions derived from this study strongly suggest that *S. aureus* biofilms resistance/tolerance towards daptomycin may be more likely related to a physiological change involving structural modifications of the membrane, which is a strain-dependent process.

Antimicrobial Agents and Chemotherapy

INTRODUCTION

Staphylococcus aureus (*S. aureus*) is a Gram-positive bacteria shown to be the most frequent cause of biofilm-associated infections (BAI) (1) and one of the major cause of morbidity and mortality in hospitals and communities (2). Unlike planktonic cells, biofilms exhibit specific phenotypic traits allowing them to resist host defenses and antibiotic treatments (3), which frequently leads to chronic infections such as endocarditis, sinusitis, and osteomyelitis but also to implant-associated infections (4).

Among the most recent clinically-used antibiotics, daptomycin is a cyclic lipopeptide approved for the treatment of serious staphylococcal infections such as bacteremia and implant-related infections (5). Daptomycin is a calcium-dependent antibiotic, acting by insertion into the Gram-positive cytoplasmic membranes where it forms oligomeric pores, causing potassium ion leakage and subsequent membrane depolarization, leading ultimately to cell death (6). As is the case for many antibiotics, daptomycin has been shown to exhibit a significant bactericidal activity against planktonic cells (7–9). However, the eradication of adherent bacteria is rarely achieved despite the large number of *in vitro* and animal studies in which daptomycin activity was evaluated (10–16). Besides the results of the literature that appear controversial (17), direct comparison between studies is not directly possible since biofilm growth and treatment protocols used greatly differ.

To get a realistic representation of daptomycin action against *S. aureus* biofilms, we developed an *in vitro* model built on the basis of our recently published *in vivo* study on *S. aureus* prosthetic vascular graft infections using the same strains (18). The interest of this approach was the possibility to use fluorescence imaging techniques that cannot be employed *in vivo* (confocal laser scanning microscopy, time-lapse and fluorescence recovery after photobleaching) to examine the penetration, diffusion, bioavailability and localization of the fluorescently-labelled antibiotic inside the biofilms. To validate this approach, we monitored for 72 h the activity of daptomycin against biofilms formed by

59 methicillin-susceptible and methicillin-resistant clinical and collection strains. In addition, we enriched
60 the culture medium with proteins and calcium to mimic the *in vivo* physiological conditions of our
61 mouse model (18). The same experiments were performed in the presence of rifampicin, an antibiotic
62 that can be combined with daptomycin for recalcitrant *S. aureus* BAI.

63

64 **MATERIALS AND METHODS**

65 **Bacterial strains**

66 Four *S. aureus* strains were tested in the present study: two of them were collection strains (methicillin-
67 susceptible *S. aureus* (MSSA) ATCC 27217 and methicillin-resistant *S. aureus* (MRSA) ATCC 33591)
68 and two others were isolated from patients with *S. aureus* bloodstream infections (MSSA 176 and
69 MRSA BCB8). All the strains were kept at -80°C in Tryptic Soy Broth (TSB; Biomérieux, France)
70 containing 20% (vol/vol) glycerol. The frozen cells were subcultured twice in TSB (one 8-hour culture
71 followed by an overnight culture) to constitute the stock cultures from which aliquots were kept at -
72 20°C. Bacterial growth and experiments were both conducted at 37°C.

73 **Antimicrobial agents and medium**

74 Daptomycin and rifampicin were both purchased from Sigma (France). The fluorescently-labelled
75 antibiotic BODIPY-FL®-daptomycin was a kind gift from Cubist Pharmaceuticals (MA, USA) and
76 BODIPY-FL® was purchased from Invitrogen (France). According to the manufacturer's instructions,
77 the stock solutions were prepared by diluting daptomycin and BODIPY®-FL-daptomycin in
78 dimethylsulfoxide (1 mg/mL), and rifampicin in sterile water (2 mg/mL), further kept at -20°C. Before
79 use, the solutions were diluted in TSB enriched with proteins (BSA, Bovine Serum Albumin, 36 g/L;
80 Sigma, France) and calcium ($CaCl_2$, $2H_2O$, 50 mg/L; Sigma, France) to mimic *in vivo* physiological
81 levels. It has been checked that, in these conditions, the final concentration of dimethylsulfoxide was

non-cytotoxic for the bacteria. Clinically-meaningful concentrations were used in this study: 20 µg/mL for both daptomycin and rifampicin. When combined, the antibiotics were mixed together before application above the biofilm surface.

Susceptibility testing

The MICs of daptomycin and rifampicin were determined by the broth microdilution method in cation-adjusted Mueller-Hinton broth (CAMHB), according to the European Committee on Antimicrobial Susceptibility Testing (EUCAST). Media were supplemented with 50 mg/L Ca^{2+} for daptomycin.

Characterization of molecular interactions between daptomycin and rifampicin by absorption and fluorescence spectroscopies

Absorption spectra of antibiotics alone and in combination were measured with a Varian's Cary® 300 spectrophotometer (Agilent Technologies, France). The corresponding fluorescence emission spectra were recorded using a Fluorolog-3 (Jobin Yvon, Inc., France) fluorescence spectrophotometer mounted with front-face detection geometry by exciting daptomycin at 360 nm. The measurements were made in quintuplicate on each sample.

***In vitro* biofilm preparation and antibiotics activities**

Biofilms were studied in a polystyrene microtiter plate-based assay since it has been shown that this material has physicochemical properties close to that of biomaterial surfaces such as polyethylene terephthalate that is used in vascular grafts (19, 20). For the preparation of *S. aureus* biofilms, 250-µL portions of an overnight subculture adjusted to an optical density of 0.02 at 600 nm (corresponding to ~10^8 CFU/mL) were added to 96-well microplates (µClear; Greiner Bio-One, France). After a 1.5-h adhesion period at 37°C, the wells were rinsed with sterile physiological water (150 mM NaCl) in order to eliminate non-adherent cells, refilled with sterile TSB enriched with proteins and calcium (TSBpc) and then incubated for 24 h at 37°C to allow biofilm growth.

Antimicrobial Agents and Chemotherapy

To assess antibiotics activities, the 24 h-biofilms were rinsed with a 150 mM NaCl aqueous solution before adding the antibiotics solutions diluted in TSBpc as described previously. Viable culturable bacteria were then counted at regular interval times: 0 h (when antibiotics are added), 24, 48 and 72 h after antibiotics injection. For each time, bacterial cultures were centrifuged 10 min at 7000*g* in order to eliminate the excess of antibiotic. The bacterial pellet was dispersed in NaCl 150 mM sterile saline solution, centrifuged again and dispersed in the same conditions. Successive decimal dilutions were then realized. For each dilution, six drops (10 µL) were deposited on Tryptic Soy Agar (TSA) plates (Biomérieux, France) and incubated at 37°C during 24 h. CFUs were counted and averaged for each dilution at each time. The detection limit of viable culturable cells was 100 CFU/mL.

Percentage of rifampicin-resistant mutants in biofilms

To measure percentages of rifampicin-resistant mutants, the antibiotics solutions (rifampicin combined or not with daptomycin) were added to 24 h-biofilms. CFUs were counted on TSA plates containing or not rifampicin (20 µg/mL) at 24 and 48 h after antibiotics injections. The percentages were obtained by calculating the ratio between the number of CFUs grown on rifampicin-containing TSA plates and the number of CFUs grown on rifampicin-free TSA plates.

Statistical analysis

The mean $\log_{10}$ CFU/mL and biovolumes for each therapy were compared with each other using ANOVA variance analyses. They were performed using the Statgraphics software (Manugistics, Rockville, USA). Significance was defined as a *P*-value associated with a Fisher test value lower than 0.05.

Confocal Laser Scanning Microscopy (CLSM)

Visualization of antibiotics activities against biofilms using Live/Dead® staining

24 h-biofilms prepared as described previously were observed 24, 48 and 72 h after antibiotics addition using a Leica TCS SP5 confocal laser scanning microscope (Leica Microsystems, France) implemented

Antimicrobial Agents and Chemotherapy

at the *Centre de Photonique Biomédicale* (CPBM, Orsay, France). Prior to each observation, bacteria were stained with 2.5 µM Syto9® (Life Technologies, France), a green cell-permeant nucleic acid dye, and 30 µM propidium iodide (PI) (Life Technologies, France), a red nucleic acid dye that can penetrate cells with compromised membranes (dead cells) only. Syto9® and PI were sequentially excited at 488 nm and 543 nm respectively and their fluorescence emissions were collected between 500 and 600 nm for Syto9® and between 640 and 750 nm for PI. Images were acquired using a 63x oil immersion objective with a 1.4 numerical aperture. The size of the confocal images was 512 x 512 pixels (82 x 82 µm²), recorded with a z-step of 1 µm. For each biofilm, four typical regions were analyzed. Images were reconstructed in 3D using ICY® Software.

Quantification of biovolumes and maximum thickness

Maximum thickness (µm) was measured directly from xyz stacks. Biovolumes (μm^3) were calculated by binarizing images with a java script executed by ICY as described previously (21). The biovolume was then defined as the overall volume of cells in the observation field. The percentage of dead cells corresponds to the ratio between biovolumes of PI-stained bacteria and Syto9®-stained bacteria.

Antibiotics penetration and localization inside biofilms

To study the penetration of BODIPY®-FL-daptomycin and its combination with rifampicin within 24 h-biofilms, we employed time-lapse microscopy, as described before (22), using the same Leica TCS SP5 confocal microscope. Briefly, the fluorescence intensity evolution over time was observed in a defined focal plane (5 µm above the substratum surface). As soon as the TSBpc-diluted solutions of BODIPY-FL®-daptomycin combined or not with rifampicin were added above the biofilm, fluorescence intensity images were acquired every second during 15 min. Simultaneously, transmission images were acquired to ensure that no structural alteration of the biofilm occurred during this process.

The labelled antibiotic was excited with a continuous argon laser line at 488 nm through a 63x oil immersion objective and the emitted fluorescence was recorded within 500 and 600 nm.

The corresponding diffusive penetration coefficients (D_p) through the biofilms were determined according to the relationship previously described by Stewart (23):

$$D_p = 1.03 \times L^2/t_{90} \quad \text{(Eq. 1)}$$

where L is the biofilm thickness and t_{90} is the time required to attain 90% of the equilibrium staining intensity at the deeper layers of the biofilm.

To observe the localization of the fluorescently-labelled daptomycin within biofilms, bacteria were counterstained with the FM4-64 dye (Life Technologies, France): this dye was also excited at 488 nm but its fluorescence emission was collected within the range 640-750 nm. The images (512 x 512 pixels) of both fluorophores were simultaneously recorded with a z-step of 1 µm.

Antibiotic diffusion and bioavailability inside biofilms using FRAP experiments

Image-based Fluorescence Recovery after Photobleaching (FRAP) measurements was used to assess local diffusion and bioavailability of the fluorescently-labelled daptomycin. Briefly, FRAP is based on a brief excitation of fluorescent molecules by a very intense light source in a user-defined region to irreversibly photobleach their fluorescence. Fluorescence recovery is then probed over time at a low light power in the same photobleached region (22, 24). All time-resolved measurements were obtained using the same confocal microscope. The time course of fluorescence intensity recovery was analyzed with mathematical models, giving access to the quantitative mobility of the fluorescent molecules and allowing to determine the diffusion coefficients. For all FRAP experiments, the fluorescence intensity image size was fixed to 512 x 128 pixels with an 80-nm pixel size and recorded using a 12-bit resolution. The line scan rate was fixed to 1400 Hz, corresponding to a total time between frames of ~ 265 ms. As determined previously, the full widths at half maximum in xy and z (along the optical axis)

Antimicrobial Agents and Chemotherapy

of the bleached profile were 0.8 µm and 14 µm, respectively, allowing to neglect diffusion along the axial/vertical axis and thus to consider only two-dimensional diffusion. Each FRAP experiment started with the acquisition of 50 images at 7% of laser maximum intensity (7 µW) followed by a 200-ms single bleached spot at 100% laser intensity. A series of 450 single section images was then collected with the laser power attenuated to its initial value (7% of the bleach intensity). The first image was recorded 365 ms after the beginning of bleaching.

RESULTS

Susceptibility testing

The MICs obtained for daptomycin and rifampicin against the four *S. aureus* strains are presented in Table 1. All isolates in planktonic conditions were susceptible to daptomycin and rifampicin. Breakpoint values of drugs according to the European Committee on Antimicrobial Susceptibility Testing (EUCAST) 2016 are: 2 mg/L for vancomycin; 1 mg/L for daptomycin; for rifampicin $S \leq 0.06$ and $R > 0.5$ mg/L.

Spectroscopic characterization of the interaction between rifampicin and daptomycin

Neither the photonic absorption properties nor the fluorescence emission spectrum of daptomycin were significantly influenced by the addition of rifampicin (Fig. 1), revealing the absence of cross-reaction between the two antibiotics.

BODIPY-FL®-daptomycin penetration, diffusion, bioavailability and localization inside *S. aureus* biofilms

Time-lapse imaging: time-lapse experiments were performed to visualize *in situ* the penetration of the fluorescently-labelled daptomycin and its combination with rifampicin throughout the deepest layers of *S. aureus* biofilms. By setting the focal plane 5 µm above the substratum surface, we demonstrated that

BODIPY-FL®-daptomycin penetrated the biofilms (~30 µm thickness) within few minutes: fluorescence intensity was measured a few seconds after antibiotic addition and increased rapidly to reach 90% of the maximal intensity in 9 min (Fig. S1 and Movie S4). The penetration coefficients obtained from Eq. 1 ranged from 2.5 ± 0.7 µm²/s for *S. aureus* 27217, 176 and 33591 to 4.9 µm²/s ± 0.7 µm²/s for *S. aureus* BCB8. These values are both of the same order by comparison with BODIPY-FL® alone for which the penetration coefficient is superior to 140 µm²/s (22). The coefficients were not statistically different in comparison with those of daptomycin in the presence of rifampicin.

FRAP imaging: FRAP was used to measure the local diffusion of BODIPY-FL®-daptomycin and its interaction with bacteria within biofilms. According to the FRAP principle (22, 24, 25), if the fluorescently-labelled daptomycin molecules are allowed to move freely in the sample, a total fluorescence recovery is observed, meaning that the fluorescence is redistributed in the defined region. Conversely, if the fluorescence recovery is not total after the photobleaching, it means that a fraction of molecules is not diffusing freely and thus interacts with its local environment. The other fraction diffuses and is thus bioavailable.

First, we checked that no bacterial movement occurred during image acquisition by representing kymograms, two-dimensional graphs of fluorescence intensity measured along a line (here a straight line drawn on the full width of the images) for each image of the FRAP series (Fig. 2a). A typical FRAP curve of BODIPY-FL®-daptomycin in *S. aureus* biofilms is presented in Fig. 2b. Whatever the bacterial strains or the treatments used (daptomycin alone and in combination with rifampicin), we demonstrated here that the fluorescence recovery was not total after photobleaching: only 20% of BODIPY-FL-®-daptomycin molecules interacted with the environment, meaning that a large excess of molecules (80%) were diffusing freely in the defined-regions and thus bioavailable (mean local diffusion coefficient, 7.1 +/- 0.6 µm²/s).

***Localization of the fluorescently-labelled daptomycin combined or not with rifampicin depending on the surrounding environment*:** As daptomycin is known to be highly bound to serum proteins (90-93%) (26), we addressed the question of whether there could be a different localization of the fluorescently-labelled daptomycin in a protein-enriched medium. As shown in Fig. 3, fluorescence intensity images were significantly different depending on the surrounding medium: regardless of the strain tested, the antibiotic appeared to be colocalized with the FM4-64 dye at the bacterial site when the surrounding medium was a NaCl aqueous solution supplemented in calcium while the antibiotic localization appeared to be mainly extracellular when the medium was enriched with proteins (TSBpc). The addition of rifampicin did not affect daptomycin localization in the biofilm.

Combining 3D-fluorescence imaging and time-kill studies to assess *S. aureus* biofilms inactivation in the presence of daptomycin alone and in association with rifampicin

We used confocal microscopy to describe the three-dimensional structures of biofilms and the temporal distribution of both live and dead cells throughout the biofilm thickness.

Fluorescence intensity images showed that the biofilms formed by the four strains yielded similar compact structures (Fig. 4a and Fig. S2 controls). Their thicknesses were neither significantly variable from one strain to another (25-29 µm, $P > 0.05$), nor between 24 h and 72 h. This is a reasonable result given that the culture medium (TSBpc) was renewed before the first observation but not over time: thus biofilm development mainly occurred during the first 24 h.

When treated with daptomycin, biofilms exhibited more free-of-cells areas compared with controls (Fig. 4a and Fig. S2). This can be related to significant decreases in biofilms thicknesses (19-21 µm in the presence of daptomycin, $P < 0.05$) by comparison with the control biofilms. Moreover, in the presence of daptomycin, no statistically significant change in the proportion of cell death over time was quantified (10-30 %, $P > 0.05$) (Fig. 4b). However, the MRSA clinical isolate (BCB8) was more

susceptible to daptomycin: ~ 60 % of cell death was quantified at 24 h, a value that decreased beyond (40% at 72 h, $P < 0.05$) due to cell regrowth (see below).

By comparison with the monotherapy treatment, the biofilms structures and thicknesses were not affected when they were treated with daptomycin in combination with rifampicin. However, in these conditions, a significantly higher proportion of cell death was observed, achieving 85% at 72 h ($P < 0.01$) (Fig. 4b). For the two MSSA strains (27217, 176) and the MRSA collection strain (33591), the antibiotics association activity gradually increased over time (Fig. 4) while the maximum activity against the MRSA clinical strain (BCB8) was reached within 24 h.

Another observation of interest (Fig. 4a) is that upon daptomycin exposure, dead cells were observed over the whole biofilm depth, including the basal layer of cells in contact with the substratum, providing further evidence of the antibiotic penetration throughout the deepest layers of the biofilms. This result is even more observable for the BCB8 strain because of the greater proportion of dead cells involved by the action of daptomycin. This process was also observed when daptomycin was used in association with rifampicin.

These data from fluorescence imaging were supported by CFU counts of suspended biofilms (Fig. 5). The results confirm that daptomycin alone was ineffective against biofilms formed by the two MSSA strains (27217, 176) and the MRSA collection strain (33591). For the MRSA clinical isolate (BCB8), only ~1-2-log reduction in bacterial counts was measured at 24 h before regrowth was observed to reach the same values as for the MSSA biofilms.

In accordance with fluorescence imaging data, the activity of the antibiotics combination was much greater than the monotherapy. The sensitivity of the microbiological method allowed determining that the cell population decreased by ~ 4 log after 72 h of treatment ($P < 0.05$). The emergence of

rifampicin-resistant mutants was verified. As presented in Fig. 6, daptomycin dramatically prevented the emergence of rifampicin-resistant mutants when used in combination.

DISCUSSION

The choice of antibiotics to treat *S. aureus* BAI remains a challenge for the medical community. In this context, the ambivalence of the published results on daptomycin activity is a relevant example. Despite increasing data about daptomycin as an option to treat implant-associated *S. aureus* infections, as many failures (18, 27) as successes (7–9, 12) have been reported both in clinical practice and in laboratory models. This highlights that *S. aureus* BAI resistance/tolerance mechanisms to antimicrobials deserve more attention.

The biofilm-associated exopolymeric matrix may be considered to act as a shield to the antimicrobial diffusion-reaction (28–32) by delaying its penetration and/or reducing its bioavailability. To verify this hypothesis non-invasively, we took advantage of dynamic fluorescence imaging methods: confocal microscopy, time-lapse imaging and FRAP. For our biofilm model and whatever the bacterial strain, no failure of daptomycin penetrability or bioavailability was observed. The opposite finding described by Siala *et al*. (31) may be related to the conditions of fluorescence acquisition that were not well-adapted to BODIPY-FL® fluorescence. In this study, time-lapse fluorescence imaging experiments demonstrated that daptomycin rapidly reached the biofilms deepest layers while section views of fluorescence intensity images presented in Fig. 3 ascertain the presence of the fluorescently-labelled antibiotic through the whole biofilm structure. Furthermore, FRAP results ascertained that only ~20% of the antibiotic molecules were immobilized. Thus, the majority of the antibiotic molecules were in free movement and could be bioavailable through the biomass (~80% of non-immobilized molecules).

We further addressed the question of whether or not daptomycin reached its bacterial target. Fluorescence intensity images provided interesting information, showing that the fluorescently-labelled antibiotic was distributed majorly in the extracellular matrix rather than in the bacterial cell membranes (Fig. 3). This is in agreement with the well-known property of daptomycin to have a very high degree of protein-binding, especially with serum albumin (90-93%) (26, 33) which is naturally present in physiological conditions. Nevertheless, the fluorescence recovery curves obtained by FRAP experiments in free medium and in the biofilms strongly suggested the reversibility of daptomycin protein-binding (33, 34): the equilibrium between the bound and unbound states may conserve the apparent mobility of the antibiotic. Additional experiments were performed in a protein-free medium (a saline solution supplemented with calcium ions). In this case, bacterial cell membranes appeared as hot spots on fluorescence images, consistently with the described antibiotic interaction with its target (6). Surprisingly, whether the medium was protein-free or not, daptomycin exhibited the same lack of effectiveness, as revealed by time-kill studies performed by fluorescent live-dead staining and conventional plating on agar (data not shown in the absence of proteins). Thus, the interaction with the matrix components cannot explain biofilm tolerance to the antibiotic.

The particular physiology of embedded bacteria should be thus considered and more specifically cells with a low metabolic activity. Previous studies using a BrdU immunofluorescent labelling technique demonstrated that the large majority of staphylococci cells in a biofilm were actually in a low-metabolic state (35, 36). Additionally, in the present study, the comparison of cell viability results obtained by CFU counts and fluorescence imaging highlighted a significant proportion of viable cells detected by Live-Dead® staining but not by CFU measurements. This subpopulation may be considered as viable but non-culturable (VBNC), a subpopulation known to have a slow metabolism (37–39). Moreover, it has been demonstrated that daptomycin is poorly effective against bacteria in stationary stage (7, 27). One can thus reasonably suggest that for bacteria with low-

Antimicrobial Agents and Chemotherapy

metabolic activity, the cell membrane dysregulation induced by daptomycin may be slower and/or more difficult to attain due to structural modifications of the cell membrane. This assumption is supported by the reported data revealing that daptomycin displays a concentration-dependent bactericidal activity against dormant cells (7, 9, 12). In the present study, we tested a double concentration of daptomycin (40 µg/mL) on the different *S. aureus* biofilms, almost leading to bactericidal effects after 24 h of drug exposure (Fig. S3) and showing no cell-regrowth over time. However, biofilm clearance was not reached. This achievement was reported to occur in a daptomycin concentration equal to or greater than 100 µg/mL but may not be relevant in clinical practice (7, 9, 12).

One particularity in this study concerns the BCB8 clinical isolate, which discriminated itself by a twice higher penetration coefficient by comparison with the other strains tested and a greater susceptibility as revealed by the observation of a larger proportion of dead cells over the whole biofilm thickness, including the basal layer in contact with the substratum. These results are in line with those obtained *in vivo* (18), which demonstrated a strain-dependent activity of daptomycin against *S. aureus* biofilms. In view of the antibiotic mechanism of action which is supposed to target the plasma membrane, the observed variable response depending on the bacterial strain may be due to a change in membrane composition or conformation from a strain to another.

Facing the lack of daptomycin efficiency in treating recalcitrant *S. aureus* BAI, the addition of rifampicin has raised great interest (10–13, 15, 40–42). Through this study, we demonstrated that the combined therapy was indeed highly efficient against *S. aureus* biofilms, but did not allow total bacterial clearance. Both antibiotics have been shown not to cross-react with each other, as evidenced by steady-state fluorescence spectroscopy. Moreover, the penetration, diffusion and localization of the fluorescently-labelled daptomycin were not affected by the presence of rifampicin. We also proved here that rifampicin-resistant mutants emerged when biofilms were treated with rifampicin alone, but not when treated with the antibiotic combination. Altogether, presented data confirm that daptomycin

prevents the emergence of rifampicin resistant mutants, allowing the bactericidal activity of rifampicin to quickly occur in time, regardless of the cell physiological state.

In conclusion, consistently with the previous *in vivo* study aiming at evaluating the antibiotic efficacy in *S. aureus* prosthetic vascular graft infections (18), we demonstrated in the present *in vitro* model a strain-dependent lack of daptomycin activity toward biofilms. Dynamic fluorescence microscopy allowed discarding a lack of antibiotic availability and interaction with bacteria. Given the mode of action of daptomycin, these observations suggest a membrane-dependent factor of tolerance in such biofilms. Therefore, to provide a better understanding of daptomycin reduced activity against biofilms, a further step should concern the analysis of the membranes composition.

FUNDING INFORMATION

This work was supported by a grant from the Ministère de l'Education Nationale, de l'Enseignement Supérieur et de la Recherche, Université Paris-Sud, for Rym Boudjemaa's PhD thesis (grant n° 2014-172).

ACKNOWLEDGEMENTS

The authors want to thank the Centre de Photonique Biomédicale (CPBM) of the Centre Laser de l'Université Paris-Sud (CLUPS/LUMAT FR2764, Orsay, France) for the confocal microscope and L2 microbiology facilities, Rachel Méallet-Renault for the spectrofluorimeter facilities at the Ecole Normale Supérieure (ENS Cachan) and Jared Silverman (Cubist Pharmaceuticals) for providing BODIPY-FL®-labelled daptomycin.

REFERENCES

1. **Sun F**, **Qu F**, **Ling Y**, **Mao P**, **Xia P**, **Chen H**, **Zhou D**. 2013. Biofilm-associated infections: antibiotic resistance and novel therapeutic strategies. Future Microbiol **8**:877–886.

2. **Costerton JW**, **Stewart PS**, **Greenberg EP**. 1999. Bacterial Biofilms: A Common Cause of Persistent Infections. Science **284**:1318–1322.

3. **Lebeaux D**, **Ghigo J-M**, **Beloin C**. 2014. Tolérance des biofilms aux antibiotiques : comprendre pour mieux traiter. J Anti-Infect **16**:112–121.

4. **Costerton JW**, **Irvin RT**, **Cheng K-J**, **Sutherland IW**. 1981. The Role of Bacterial Surface Structures in Pathogenesis. Crit Rev Microbiol **8**:303–338.

5. **Steenbergen JN**, **Alder J**, **Thorne GM**, **Tally FP**. 2005. Daptomycin: a lipopeptide antibiotic for the treatment of serious Gram-positive infections. J Antimicrob Chemother **55**:283–288.

6. **Straus SK**, **Hancock REW**. 2006. Mode of action of the new antibiotic for Gram-positive pathogens daptomycin: Comparison with cationic antimicrobial peptides and lipopeptides. Biochim Biophys Acta BBA - Biomembr **1758**:1215–1223.

7. **Mascio CTM**, **Alder JD**, **Silverman JA**. 2007. Bactericidal Action of Daptomycin against Stationary-Phase and Nondividing Staphylococcus aureus Cells. Antimicrob Agents Chemother **51**:4255–4260.

8. **Cotroneo N**, **Harris R**, **Perlmutter N**, **Beveridge T**, **Silverman JA**. 2008. Daptomycin exerts bactericidal activity without lysis of Staphylococcus aureus. Antimicrob Agents Chemother **52**:2223–2225.

9. **Silverman JA**, **Perlmutter NG**, **Shapiro HM**. 2003. Correlation of Daptomycin Bactericidal Activity and Membrane Depolarization in Staphylococcus aureus. Antimicrob Agents Chemother **47**:2538–2544.

10. **Khasawneh FA**, **Ashcraft DS**, **Pankey GA**. 2008. In vitro testing of daptomycin plus rifampin against methicillin-resistant Staphylococcus aureus resistant to rifampin. Saudi Med J **29**:1726–1729.

11. **LaPlante KL**, **Woodmansee S**. 2009. Activities of Daptomycin and Vancomycin Alone and in Combination with Rifampin and Gentamicin against Biofilm-Forming Methicillin-Resistant Staphylococcus aureus Isolates in an Experimental Model of Endocarditis. Antimicrob Agents Chemother **53**:3880–3886.

12. **Parra-Ruiz J**, **Vidaillac C**, **Rose WE**, **Rybak MJ**. 2010. Activities of High-Dose Daptomycin, Vancomycin, and Moxifloxacin Alone or in Combination with Clarithromycin or Rifampin in a Novel In Vitro Model of Staphylococcus aureus Biofilm. Antimicrob Agents Chemother **54**:4329–4334.

13. **Olson ME**, **Slater SR**, **Rupp ME**, **Fey PD**. 2010. Rifampicin enhances activity of daptomycin and vancomycin against both a polysaccharide intercellular adhesin (PIA)-dependent and -independent Staphylococcus epidermidis biofilm. J Antimicrob Chemother **65**:2164–2171.

14. **Nadrah K**, **Strle F**. 2011. Antibiotic Combinations with Daptomycin for Treatment of *Staphylococcus aureus* Infections. Chemother Res Pract **2011**:e619321.

15. **Cirioni O**, **Mocchegiani F**, **Ghiselli R**, **Silvestri C**, **Gabrielli E**, **Marchionni E**, **Orlando F**, **Nicolini D**, **Risaliti A**, **Giacometti A**. 2010. Daptomycin and Rifampin Alone and in Combination Prevent Vascular Graft Biofilm Formation and Emergence of Antibiotic Resistance

399 in a Subcutaneous Rat Pouch Model of Staphylococcal Infection. Eur J Vasc Endovasc Surg
400 **40**:817–822.

401 16. **Salem AH**, **Elkhatib WF**, **Noreddin AM**. 2011. Pharmacodynamic assessment of vancomycin–
402 rifampicin combination against methicillin resistant Staphylococcus aureus biofilm: a parametric
403 response surface analysis. J Pharm Pharmacol **63**:73–79.

404 17. **John A-K**, **Schmaler M**, **Khanna N**, **Landmann R**. 2011. Reversible Daptomycin Tolerance of
405 Adherent Staphylococci in an Implant Infection Model. Antimicrob Agents Chemother **55**:3510–
406 3516.

407 18. **Revest M, Jacqueline C, Boudjemaa R, Caillon J, Le Mabecque V, Breteche A, Steenkeste K,**
408 **Tattevin P, Potel G, Michelet C, Fontaine-Aupart MP, Boutoille D**. 2016. New in vitro and in
409 vivo models to evaluate antibiotic efficacy in Staphylococcus aureus prosthetic vascular graft
410 infection. J Antimicrob Chemother, in press.

411 19. **Wang IW**, **Anderson JM**, **Jacobs MR**, **Marchant RE**. 1995. Adhesion of Staphylococcus
412 epidermidis to biomedical polymers: contributions of surface thermodynamics and hemodynamic
413 shear conditions. J Biomed Mater Res **29**:485–493.

414 20. **Mafu AA**, **Plumety C**, **Deschênes L**, **Goulet J**. 2010. Adhesion of Pathogenic Bacteria to Food
415 Contact Surfaces: Influence of pH of Culture. Int J Microbiol **2011**:e972494.

416 21. **Sanchez-Vizuete P**, **Coq DL**, **Bridier A**, **Herry J-M**, **Aymerich S**, **Briandet R**. 2015.
417 Identification of ypqP as a New Bacillus subtilis Biofilm Determinant That Mediates the
418 Protection of Staphylococcus aureus against Antimicrobial Agents in Mixed-Species
419 Communities. Appl Environ Microbiol **81**:109–118.

22. **Daddi Oubekka S**, **Briandet R**, **Fontaine-Aupart M-P**, **Steenkeste K**. 2012. Correlative time-resolved fluorescence microscopy to assess antibiotic diffusion-reaction in biofilms. Antimicrob Agents Chemother **56**:3349–3358.

23. **Stewart PS**. 2003. Diffusion in Biofilms. J Bacteriol **185**:1485–1491.

24. **Daddi Oubekka S, Briandet R, Waharte F, Fontaine-Aupart M-P, Steenkeste K.** 2011. Image-based fluorescence recovery after photobleaching (FRAP) to dissect vancomycin diffusion-reaction processes in Staphylococcus aureus, Proc. SPIE 8087, Clinical and Biomedical Spectroscopy and Imaging II, p. 80871I–80871I–7.

25. **Bridier A**, **Tischenko E**, **Dubois-Brissonnet F**, **Herry J-M**, **Thomas V**, **Daddi-Oubekka S**, **Waharte F**, **Steenkeste K**, **Fontaine-Aupart M-P**, **Briandet R**. 2011. Deciphering biofilm structure and reactivity by multiscale time-resolved fluorescence analysis. Adv Exp Med Biol **715**:333–349.

26. **Benvenuto M**, **Benziger DP**, **Yankelev S**, **Vigliani G**. 2006. Pharmacokinetics and Tolerability of Daptomycin at Doses up to 12 Milligrams per Kilogram of Body Weight Once Daily in Healthy Volunteers. Antimicrob Agents Chemother **50**:3245–3249.

27. **Humphries RM**, **Pollett S**, **Sakoulas G**. 2013. A Current Perspective on Daptomycin for the Clinical Microbiologist. Clin Microbiol Rev **26**:759–780.

28. **Pibalpakdee P**, **Wongratanacheewin S**, **Taweechaisupapong S**, **Niumsup PR**. 2012. Diffusion and activity of antibiotics against Burkholderia pseudomallei biofilms. Int J Antimicrob Agents **39**:356–359.

29. **Singh R**, **Ray P**, **Das A**, **Sharma M**. 2010. Penetration of antibiotics through Staphylococcus aureus and Staphylococcus epidermidis biofilms. J Antimicrob Chemother **65**:1955–1958.

30. **Jefferson KK**, **Goldmann DA**, **Pier GB**. 2005. Use of Confocal Microscopy To Analyze the Rate of Vancomycin Penetration through Staphylococcus aureus Biofilms. Antimicrob Agents Chemother **49**:2467–2473.

31. **Siala W**, **Mingeot-Leclercq M-P**, **Tulkens PM**, **Hallin M**, **Denis O**, **Bambeke FV**. 2014. Comparison of the Antibiotic Activities of Daptomycin, Vancomycin, and the Investigational Fluoroquinolone Delafloxacin against Biofilms from Staphylococcus aureus Clinical Isolates. Antimicrob Agents Chemother **58**:6385–6397.

32. **Stewart PS**, **Davison WM**, **Steenbergen JN**. 2009. Daptomycin Rapidly Penetrates a Staphylococcus epidermidis Biofilm. Antimicrob Agents Chemother **53**:3505–3507.

33. **Zeitlinger MA**, **Derendorf H**, **Mouton JW**, **Cars O**, **Craig WA**, **Andes D**, **Theuretzbacher U**. 2011. Protein Binding: Do We Ever Learn? Antimicrob Agents Chemother **55**:3067–3074.

34. **Schmidt S**, **Röck K**, **Sahre M**, **Burkhardt O**, **Brunner M**, **Lobmeyer MT**, **Derendorf H**. 2008. Effect of Protein Binding on the Pharmacological Activity of Highly Bound Antibiotics. Antimicrob Agents Chemother **52**:3994–4000.

35. **Oubekka SD**. 2012. Dynamique réactionnelle d'antibiotiques au sein des biofilms de Staphylococcus aureus : apport de la microscopie de fluorescence multimodale. Ph.D. Thesis, Université Paris Sud - Paris XI, France.

36. **Rani SA**, **Pitts B**, **Beyenal H**, **Veluchamy RA**, **Lewandowski Z**, **Davison WM**, **Buckingham-Meyer K**, **Stewart PS**. 2007. Spatial Patterns of DNA Replication, Protein Synthesis, and

461 Oxygen Concentration within Bacterial Biofilms Reveal Diverse Physiological States. J Bacteriol
462 **189**:4223–4233.

463 37. **Ayrapetyan M**, **Williams TC**, **Oliver JD**. 2014. Bridging the gap between viable but non-
464 culturable and antibiotic persistent bacteria. Trends Microbiol **23**:7–13.

465 38. **Li L**, **Mendis N**, **Trigui H**, **Oliver JD**, **Faucher SP**. 2014. The importance of the viable but non-
466 culturable state in human bacterial pathogens. Microb Physiol Metab **5**:258.

467 39. **Pasquaroli S**, **Citterio B**, **Cesare AD**, **Amiri M**, **Manti A**, **Vuotto C**, **Biavasco F**. 2014. Role of
468 Daptomycin in the Induction and Persistence of the Viable but Non-Culturable State of
469 Staphylococcus Aureus Biofilms. Pathogens **3**:759–768.

470 40. **Credito K**, **Lin G**, **Appelbaum PC**. 2007. Activity of Daptomycin Alone and in Combination
471 with Rifampin and Gentamicin against Staphylococcus aureus Assessed by Time-Kill
472 Methodology. Antimicrob Agents Chemother **51**:1504–1507.

473 41. **Garrigós C**, **Murillo O**, **Euba G**, **Verdaguer R**, **Tubau F**, **Cabellos C**, **Cabo J**, **Ariza J**. 2010.
474 Efficacy of Usual and High Doses of Daptomycin in Combination with Rifampin versus
475 Alternative Therapies in Experimental Foreign-Body Infection by Methicillin-Resistant
476 Staphylococcus aureus. Antimicrob Agents Chemother **54**:5251–5256.

477 42. **Stein C, Makarewicz O, Forstner C, Weis S, Hagel S, Löffler B, Pletz MW**. 2016. Should
478 daptomycin–rifampin combinations for MSSA/MRSA isolates be avoided because of
479 antagonism? Infection, in press.

480

Antibiotic	MSSA ATCC 27217	MSSA 176	MRSA ATCC 33591	MRSA BCB8
Daptomycin	0.25	0.5	0.25	0.125
Rifampicin	< 0.06	0.015	0.0075	< 0.06

481 **Table 1:** MICs (mg/L) of daptomycin and rifampicin against the four *S. aureus* strains (± 5%).

482

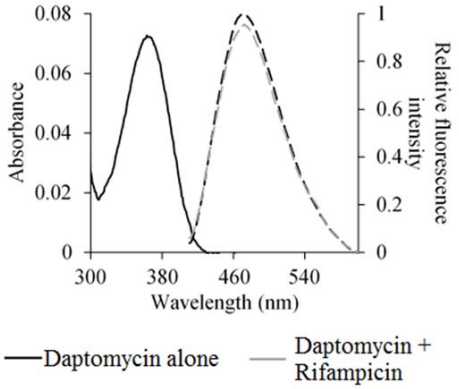

483

484 **Fig. 1:** Absorption (straight lines) and fluorescence spectra (dashed lines) of daptomycin (20 µg/mL)

485 alone and combined to rifampicin (20 µg/mL). Excitation wavelength: 360 nm. Daptomycin alone is

486 represented in black and its combination with rifampicin in grey.

487

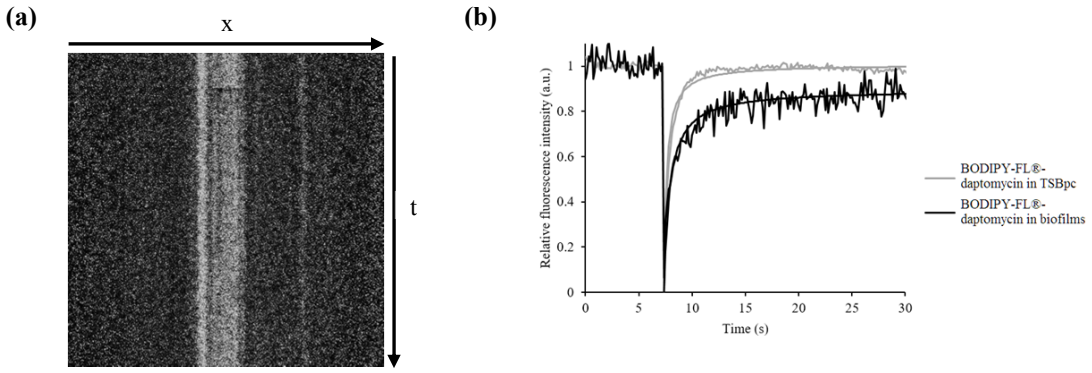

488 **Fig. 2:** FRAP acquisitions for BODIPY-FL®-daptomycin inside *S. aureus* biofilms. **(a)** Kymogram
489 representation (x,t) of FRAP acquisitions. The line along which the kymogram was done is 38 µm. **(b)**
490 Typical fluorescence recovery curves representative of six different zones for each condition:
491 BODIPY-FL®-daptomycin inside biofilms (black) and inside TSBpc without biofilm (grey). The
492 kymogram and fluorescence recovery curve presented here are the ones obtained for MSSA 27217
493 biofilms since they were representative of the data obtained for the other strains only in the presence or
494 not of rifampicin.

495

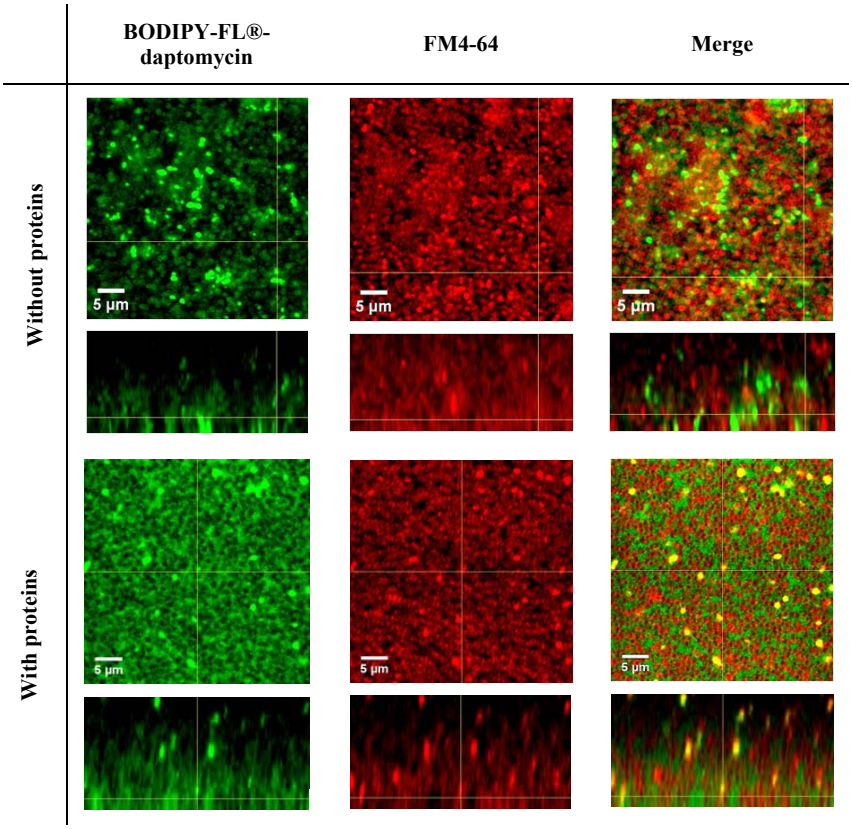

Fig. 3: Fluorescence imaging of BODIPY-FL®-daptomycin (green channel) and FM4-64 (red channel) in *S. aureus* biofilms. Merged images are also shown. On the top, the surrounding medium is a NaCl (150 mM) aqueous solution supplemented with calcium ions (50 mg/L). On the bottom, the surrounding medium is TSB enriched with proteins (36 g/L) and calcium ions (50 mg/L). Only images of MSSA 27217 biofilms are represented since they were representative of all biofilms visualized for other strains in the presence or not of rifampicin.

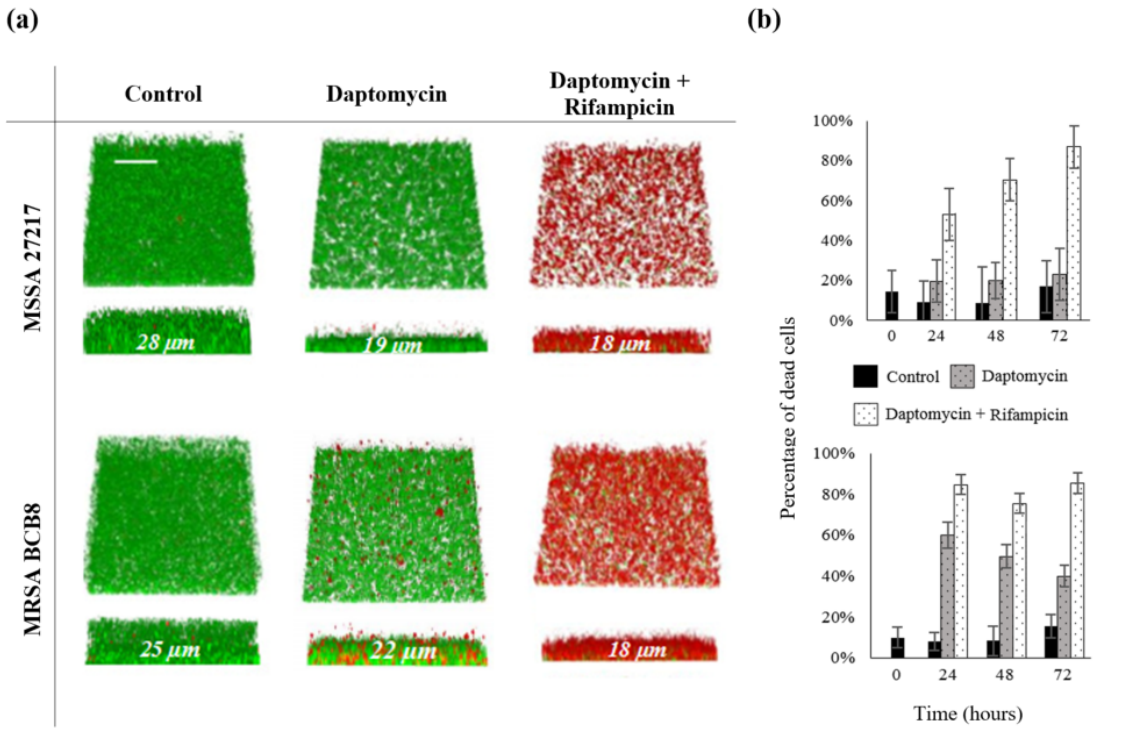

Fig. 4: (a) Visualization of MSSA 27217 and MRSA BCB8 biofilms using 3D reconstruction to observe biofilm thickness. Images were collected without any drug exposure (control) and after 72 h exposure to unlabeled daptomycin (20 µg/mL) alone and in association with rifampicin (20 µg/mL). Dead cells were stained red with propidium iodide and all bacteria were stained green with Syto9®. The acquisition was performed on the whole biofilm thickness with an axial displacement of 1 µm. Images dimension is 82x82µm². The scale bar corresponds to 20 µm and mean thickness values of the biofilms over time (from 24 to 72 h) are written in white on each image. **(b)** Percentage of dead cells evolution over time calculated from three series of biofilms images treated or not with daptomycin (20 µg/mL) alone or in combination with rifampicin (20 µg/mL). Black bars, controls; grey bars, daptomycin alone; open bars, daptomycin-rifampicin combination. Error bars represent the standard deviation.

516

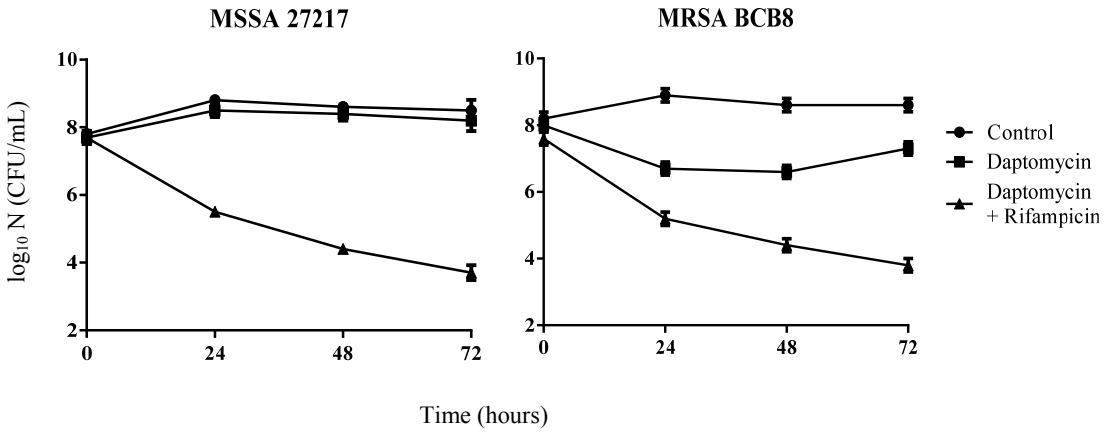

517

518 **Fig. 5:** Time-kill curves of daptomycin (20 µg/mL) activities combined or not with rifampicin (20
519 µg/mL) against MSSA 27217 and MRSA BCB8 biofilms. Filled circles: controls; filled squares:
520 daptomycin; filled triangles: daptomycin + rifampicin. Error bars represent the standard deviation.

521

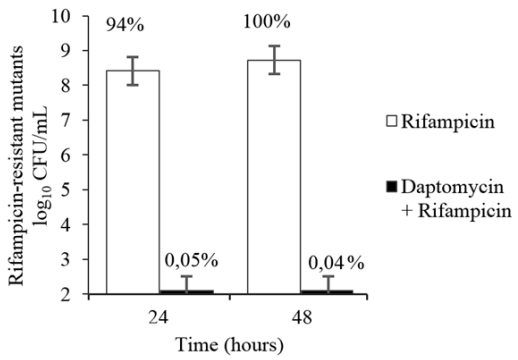

522

523 **Fig. 6:** Number of rifampicin-resistant mutants determined in MSSA 27217 biofilms counted on
524 rifampicin-containing TSA plates. Above each bar is shown the percentage of rifampicin-resistant
525 mutants in *S. aureus* biofilms among the total bacterial population. Error bars represent the standard
526 deviation. White bars, rifampicin alone (20 µg/mL); black bars, daptomycin-rifampicin combination
527 (20 µg/mL for both antibiotics).

528

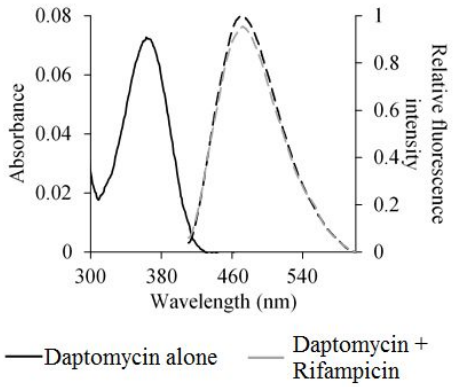

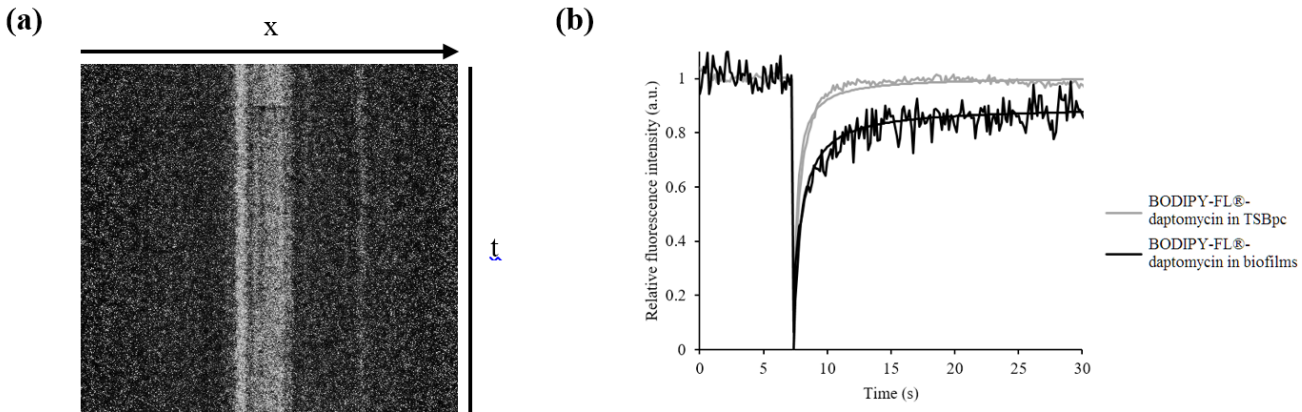

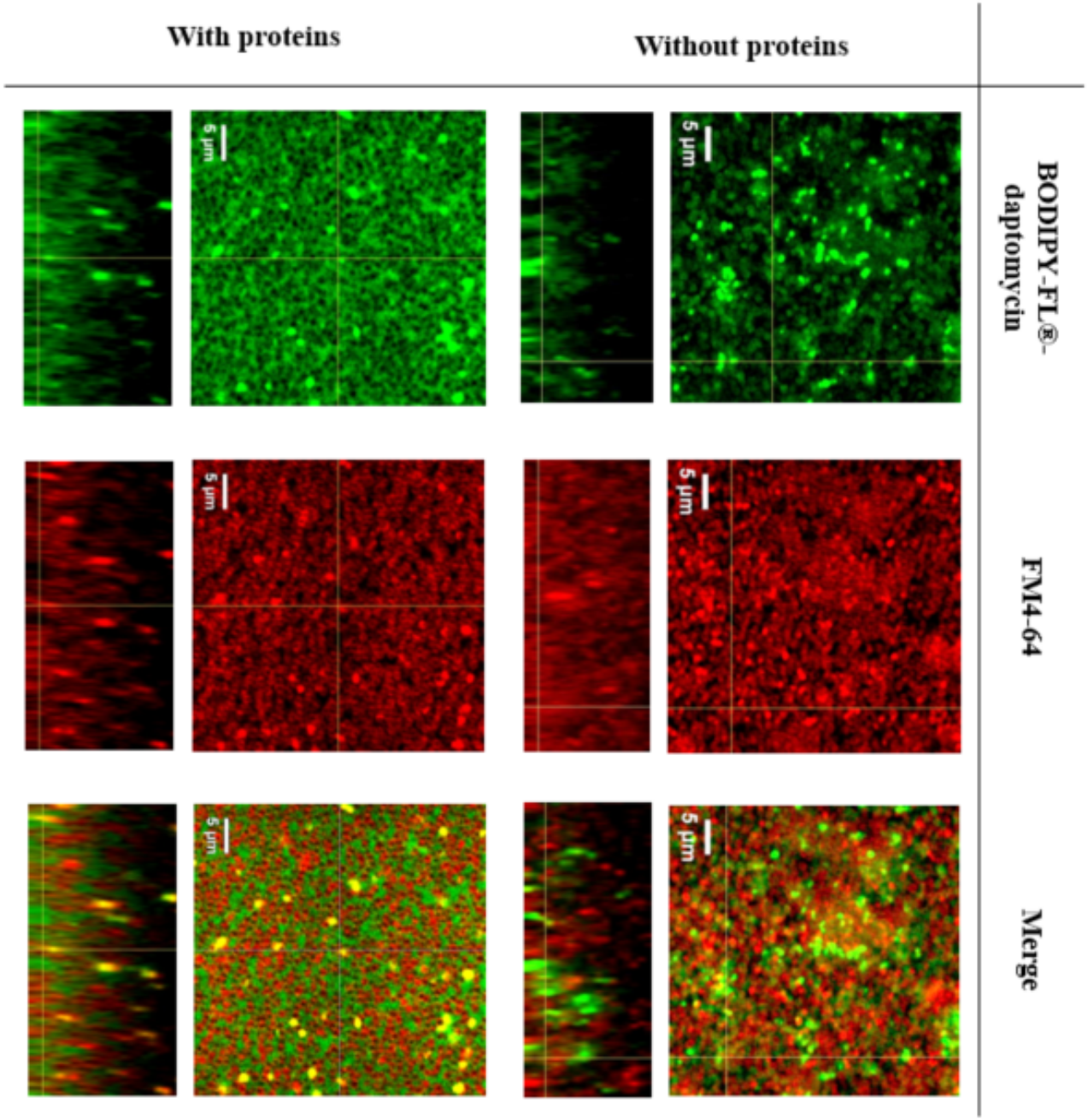
With proteins
Without proteins
BODIPY-FL®-daptomycin
FM4-64
Merge
5 µm